Electronic Supplementary Information to

Branched electron-donor core effect in D-π-A star-shaped small molecules on their properties and performance in single-component and bulk-heterojunction organic solar cells

Alexander N. Solodukhin[1], Yuriy N. Luponosov[1]*, Artur L. Mannanov[1,2], Petr S. Savchenko[1], Artem V. Bakirov[1,3], Maxim A. Shcherbina[1,4], Sergei N. Chvalun[1,3], Dmitry Yu. Paraschuk[1,2]*, Sergey A. Ponomarenko[1]

[1]Enikolopov Institute of Synthetic Polymeric Materials of the Russian Academy of Sciences, Profsoyuznaya st. 70, Moscow 117393, Russia

[2]Faculty of Physics, Lomonosov Moscow State University, Leninskie Gory 1/62, Moscow 119991, Russia

[3]National Research Centre Kurchatov Institute, 1 ak. Kurchatov square, 123098 Moscow, Russian Federation

[4] Moscow Institute of Physics and Technology, 9 Institutsky line, Dolgoprudny, Moscow region, 141700, Russian Federation.

‡ A. N. Solodukhin and Yu. N. Luponosov contributed equally to this work

*Corresponding authors e-mail: luponosov@ispm.ru (Yu. N. Luponosov); paras@physics.msu.ru (D. Yu. Paraschuk);

CONTENTS

1. Experimental part

1.1 Materials

Tetra*kis*(triphenylphosphine)palladium (0) $Pd(PPh_3)_4$, malononitrile were obtained from Sigma–Aldrich Co. and used without further purification. THF, toluene, hexane, pyridine were dried and purified according to the known techniques and then used as solvents. *Tris*(4-bromo-2-methoxyphenyl)amine (**1a**) was obtained as described in Ref. [1]. 2,6,10-tribromo-4,4,8,8,12,12-hexa*kis*(4-methylphenyl)-4*H*,8*H*,12*H*-benzo [1,9]quinolizino[3,4,5,6,7-*defg*]acridine (**1b**) was obtained as described in Ref. [2]. 2-hexyl-5,5-dimethyl-2-[5'-(4,4,5,5-tetramethyl-1,3,2-dioxaborolan-2-yl)-2,2'-bithien-5-yl]-1,3-dioxane (**2**) was obtained as described in Ref. [3]. All reactions, unless stated otherwise, were carried out under an inert atmosphere.

1.2 Characterization

^{1}H NMR spectra were recorded at a "Bruker WP-250 SY "spectrometer, working at a frequency of 250.13 MHz and utilizing $CDCl_3$ signal (7.25 ppm) as the internal standard. ^{13}C NMR spectra were recorded using a "Bruker Avance II 300" spectrometer at 75 MHz. In the case of ^{1}H NMR spectroscopy, the compounds to be analyzed were taken in the form of 1% solutions in $CDCl_3$. In the case of ^{13}C NMR spectroscopy, the compounds to be analyzed were taken in the form of 5% solutions in $CDCl_3$. The spectra were then processed using the ACD Labs software.

Elemental analysis of C, N and H elements was carried out using a CHN automatic analyzer (CE 1106). The settling titration using $BaCl_2$ was applied to analyze Sulfur. The experimental error for elemental analysis is 0.30-0.50%. Knövenagel condensation was carried out in the microwave (Discovery, CEM corporation), using a standard method with the open vessel option, 50 watts. In the case of column chromatography, silica gel 60 (Merck) was taken. Absorption profiles were recorded with an absorption spectrometer (Shimadzu UV 2501 PC). Optical absorption were recorded at room temperature in diluted THF solutions (10^{-5} M) and films cast from THF solutions with concentration 10 g/L on quartz substrates.

Cyclic voltammetry measurements were carried out using solid compact layers of the oligomers, which in turn were made by electrostatically rubbing the materials onto a glassy carbon electrode using IPC-Pro M potentiostat. Measurements were made in acetonitrile solution using 0.1 M Bu_4NPF_6 as supporting electrolyte. The scan rate was 200 mV s^{-1}. The glassy carbon electrode was used as a work electrode. Potentials were measured relative to a saturated calomel electrode (SCE). The highest occupied molecular orbital (HOMO) and the lowest unoccupied molecular orbital (LUMO) energies were evaluated using the first standard oxidation (φ_{ox}) and reduction (φ_{red}) potentials obtained from CV experiments as $E(HOMO) = -e(\varphi_{ox}+4.40)$(eV) and $E(LUMO) = -e(\varphi_{red}+4.40)$(eV), where e is the elementary charge [4,5].

Thermogravimetric analysis was carried out in a dynamic mode within the temperature range of 30–700 °C using a "Mettler Toledo TG50" system equipped with a microbalance (M3). Heating/cooling rate was chosen to be 10 °C/min. Every compound was studied in air and nitrogen flow of 200 mL/min. Differential scanning calorimetry (DSC) scans were obtained with a "Mettler Toledo DSC30" system with 20 °C/min heating/cooling rate in the temperature range of +20–290 °C for all compounds. N_2 flow of 50 mL/min was used.

The solubility of molecules was measured using their saturated solutions in 1,2-dichlorobenzene, which were prepared by stirring of an excess of solid material in the solvent. For this purpose, the compounds were added in small portions to 1 mL of pure solvent. As prepared, the saturated solution was filtered through 0.25-mm PTFE syringe filters, and the solvent was evaporated using a rotary evaporator. Afterwards the residue was dried in vacuum at 130°C until reaching its constant weight, which was used to calculate the solubility value.

1.3 Synthetic procedures.

***tris*{4-[5'-(2-hexyl-5,5-dimethyl-1,3-dioxan-2-yl)-2,2'-bithien-5-yl]-2-methoxyphenyl}amine (3a)**. In an inert atmosphere, degassed solutions of *tris*(4-bromo-2-methoxyphenyl)amine (**1a**) (0.65 g, 1.1 mmol) and 2-hexyl-5,5-dimethyl-2-[5'-(4,4,5,5-tetramethyl-1,3,2-dioxaborolan-2-yl)-2,2'-bithien-5-yl]-1,3-dioxane **2** (2.0 g, 4.4 mmol) in toluene/ethanol mixture (50/5 mL) and 2M solution of aq. Na_2CO_3 (6.1 mL) were added to $Pd(PPh_3)_4$ (142 mg, 0.1 mmol). The reaction mixture was stirred under reflux for 9 h, and then it was cooled to room temperature and poured into 75 mL of water and 50 mL of toluene. The organic phase was separated, washed with water, dried over sodium sulfate and filtered. The solvent was evaporated in vacuum and the residue was dried at 1 Torr. The product was purified by column chromatography on silica gel (eluent toluene : hexane, 1 : 1) to give pure compound **3a** (1.37 g, 85%) as yellow solid. ^{1}H NMR (250 MHz, Acetone-d6): δ [ppm] 0.63 (s, 9H), 0.84 (t, 9H, *J* =6.7 Hz), 1.18 (s, 9H), 1.20-1.27 (overlapping peaks, 18H), 1.38-1.48 (overlapping peaks, 6H), 1.77-1.86 (overlapping peaks, 6H), 3.41 (d, 6H, *J* =11.0 Hz), 3.66 (s, 9H), 3.69 (d, 6H, *J* =11.3 Hz), 6.85 (d, 3H, *J* =8.2 Hz), 6.88 (d, 3H, *J* =3.7 Hz), 7.11-7.16 (overlapping peaks, 6H), 7.19 (d, 3H, *J* =3.7 Hz), 7.25 (d, 3H, *J* =1.9 Hz), 7.32 (d, 3H, *J* =3.8 Hz). ^{13}C NMR (125 MHz, Acetone-d6): δ [ppm] 13.43, 21.11, 22.09, 22.34, 22.95, 29.10, 31.65, 44.81, 55.70, 71.39, 99.93, 110.61, 118.25, 123.12, 123.49, 124.57, 125.17, 127.10, 129.83, 135.62, 137.12, 137.37, 143.06, 143.67, 153.72. Calcd (%) for $C_{81}H_{99}NO_9S_6$: C, 68.37; H, 7.01; S, 13.52; N, 0.98. Found C, 68.48; H, 7.14; S, 13.41; N, 0.95.

2,6,10-*tris*[5'-(2-hexyl-5,5-dimethyl-1,3-dioxan-2-yl)-2,2'-bithien-5-yl]-4,4,8,8,12,12-hexakis(4-methylphenyl)-4*H*,8*H*,12*H*-benzo[1,9]quinolizino[3,4,5,6,7-*defg*]acridine (3b). This compound was obtained according to the procedure described for **3a** using 2,6,10-tribromo-

4,4,8,8,12,12-hexa*kis*(4-methylphenyl)-4*H*,8*H*,12*H*-benzo [1,9]quinolizino[3,4,5,6,7-*defg*]acridine **1b** (1.5 g, 1.4 mmol), 2-hexyl-5,5-dimethyl-2-[5'-(4,4,5,5-tetramethyl-1,3,2-dioxaborolan-2-yl)-2,2'-bithien-5-yl]-1,3-dioxane **2** (2.78 g, 5.7 mmol), $Pd(PPh_3)_4$ (164 мг, 0.1 mmol), toluene (40 mL), ethanol (4 mL), 2M solution of aq. Na_2CO_3 (8.5 mL). The reaction mixture was stirred under reflux for 9 h, and then it was cooled to room temperature and poured into 50 mL of water and 50 mL of toluene. The organic phase was separated, washed with water, dried over sodium sulfate and filtered. The solvent was evaporated in vacuum and the residue was dried at 1 Torr. The product was purified by column chromatography on silica gel (eluent toluene : hexane, 1 : 1) to give pure compound **3b** (2.0 g, 74%) as yellow solid. ^{1}H NMR (250 MHz, Acetone-d6): δ [ppm] 0.62 (s, 9H), 0.83 (t, 9H, *J* =6.8 Hz), 1.17 (s, 9H), 1.21-1.29 (overlapping peaks, 18H), 1.36-1.46 (overlapping peaks, 6H), 1.76-1.84 (overlapping peaks, 6H), 2.31 (s, 18H), 3.38 (d, 6H, *J* =11.2 Hz), 3.65 (d, 6H, *J* =11.0 Hz), 6.76-6.85 (overlapping peaks, 18H), 6.96-7.03 (overlapping peaks, 15H), 7.03 (d, 3H, *J* =3.7 Hz), 7.19 (s, 6H). ^{13}C NMR (125 MHz, Acetone-d6): δ [ppm] 13.29, 20.07, 21.06, 22.04, 22.24, 22.86, 24.16, 29.32, 31.56, 44.65, 55.37, 71.39, 99.94, 123.10, 123.23, 124.62, 125.06, 126.97, 128.38. 128.44, 129.60, 129.87, 134.29, 135.85, 135.92, 137.04, 142.50, 142.57, 144.00. Calcd (%) for $C_{123}H_{129}NO_6S_6$: C, 77.36; H, 6.81; S, 10.07; N, 0.73. Found C, 77.48; H, 6.95; S, 10.14; N, 0.71.

1,1',1''-{nitrilo*tris*[(3-methoxy-4,1-phenylene)-2,2'-bithiene-5',5-diyl]}triheptan-1-one (4a). 1M HCl (1.1 mL) was added to a solution of compound **3a** (0.8 g, 0.6 mmol) in THF (15 mL) and then the reaction mixture was stirred for 4 hours at reflux at boiling temperature. After completion of the reaction the organic phase was separated using diethyl ether, washed with water and filtered off to give pure compound **4a** (0.58 g, 88%) as orange powder. ^{1}H NMR (250 MHz, $CDCl_3$): δ [ppm] 0.88 (t, 9H, *J* =6.7 Hz), 1.27-1.41 (overlapping peaks, 18H), 1.68-1.79 (overlapping peaks, 6H), 1.77-1.86 (overlapping peaks, 6H), 2.86 (t, 6H, *J* =7.3 Hz), 3.67 (s, 9H), 6.87 (d, 3H, *J* =8.9 Hz), 7.07-7.12 (overlapping peaks, 6H), 7.17 (d, 3H, *J* =4.0 Hz), 7.20 (d, 3H, *J* =4.0 Hz), 7.27 (d, 3H, *J* =3.7 Hz), 7.60 (d, 3H, *J* =4.0 Hz). Calcd (%) for $C_{66}H_{69}NO_6S_6$: C, 68.07; H, 5.97; S, 16.52; N, 1.20. Found C, 68.16; H, 6.09; S, 16.59; N, 1.16.

1,1',1''-[[4,4,8,8,12,12-hexakis(4-methylphenyl)-4*H*,8*H*,12*H*-benzo[1,9]quinolizino[3,4,5,6,7-*defg*]acridine-2,6,10-triyl]*tris*(2,2'-bithiene-5',5-diyl)]triheptan-1-one (4b). This compound was obtained according to the procedure described for **4a** using compound **3b** (1.6 g, 0,1 mmol), 1M HCl (4.1 mL), THF (20 mL). After completion of the reaction the organic phase was separated using diethyl ether, washed with water and filtered off to give pure compound **4b** (1.24 g, 90%) as an orange powder. ^{1}H NMR (250 MHz, $CDCl_3$): δ [ppm] 0.89 (t, 9H, *J* =6.6 Hz), 1.28-1.43 (overlapping peaks, 18H), 1.68-1.79 (overlapping peaks, 6H), 2.34 (s, 9H), 2.84 (t, 6H, *J* =7.5 Hz),

6.71 (d, 12H, *J* =8.1 Hz), 6.80 (d, 3H, *J* =3.8 Hz), 6.91 (d, 12H, *J* =8.2 Hz), 7.07 (d, 3H, *J* =4.0 Hz), 7.12 (s, 6H), 7.14 (d, 3H, *J* =3.8 Hz), 7.55 (d, 3H, *J* =4.1 Hz). ^{13}C NMR (125 MHz, $CDCl_3$): δ [ppm] 14.02, 20.97, 22.48, 24.90, 28.99, 31.58, 38.97, 55.27, 123.23, 123.67, 125.16, 126.42, 128.08, 128.37, 129.49, 129.92, 132.51, 134.52, 134.70, 135.70, 142.00, 142.20, 145.30, 145.35, 193.14. Calcd (%) for $C_{108}H_{99}NO_3S_6$: C, 78.55; H, 6.04; S, 11.65; N, 0.85. Found C, 78.71; H, 6.26; S, 11.52; N, 0.83.

***tris*{4-[5'-(1,1-dicyanooct-1-en-2-yl)-2,2'-bithien-5-yl]-2-methoxyphenyl}amine (m-TPA).** Compound **4a** (0.53 g, 0.5 mmol), malononitrile (0.45 g, 6.8 mmol) and dry pyridine (12.0 mL) were placed in a reaction vessel and stirred under argon atmosphere for 11 hours at reflux using the microwave heating. After completeness of the reaction, pyridine was evaporated in vacuum and the residue was dried at 1 Torr. The crude product was purified by column chromatography on silica gel (eluent methylene chloride). Further purification included precipitation of the product from its THF solution with toluene and hexane to give pure product as a black solid (0.3 g, 51%). ^{1}H NMR (250 MHz, $CDCl_3$): δ [ppm] 0.93 (t, 9H, *J* =7.0 Hz), 1.32-1.41 (overlapping peaks, 12H), 1.45-1.55 (overlapping peaks, 6H), 1.68-1.79 (overlapping peaks, 6H), 2.94 (t, 6H, *J* =7.6 Hz), 3.70 (s, 9H), 6.93 (d, 3H, *J* =8.8 Hz), 7.13-7.18 (overlapping peaks, 6H), 7.25 (d, 3H, *J* =4.0 Hz), 7.28 (d, 3H, *J* = 4.3 Hz), 7.35 (d, 3H, *J* =4.0 Hz), 7.95 (d, 3H, *J* =4.3 Hz). ^{13}C NMR (125 MHz, $CDCl_3$): δ [ppm] 13.82, 22.35, 29.13, 30.36, 31.23, 37.49, 56.20, 76.76, 110.78, 113.77, 114.59, 118.79, 123.74, 124.67, 125.18, 127.51, 129.61, 133.66, 135.00, 135.20, 137.51, 146.77, 147.00, 153.58, 166.23. Calcd (%) for $C_{75}H_{69}N_7O_3S_6$: C, 68.83; H, 5.31; S, 14.70; N, 7.49. Found C, 68.96; H, 5.42; S, 14.77; N, 7.43.

2,2',2''-[[4,4,8,8,12,12-hexakis(4-methylphenyl)-4H,8H,12H-benzo[1,9]quinolizino[3,4,5,6,7-*defg*]acridine-2,6,10-triyl]tris(2,2'-bithiene-5',5-diylhept-1-yl-1-ylidene)]trimalononitrile (f-TPA). This compound was obtained according to the procedure described for **m-TPA** using compound **4b** (1.1 g, 0.7 mmol), malonitrile (0.31 g, 4.7 mmol), and pyridine (17 mL). The crude product was purified by column chromatography on silica gel (eluent methylene chloride). Further purification included precipitation of the product from its THF solution with toluene and hexane to give pure product as a black solid (0.84 g, 70%). ^{1}H NMR (250 MHz, $CDCl_3$): δ [ppm] 0.92 (t, 9H, *J* =7.1 Hz), 1.31-1.39 (overlapping peaks, 12H), 1.43-1.54 (overlapping peaks, 6H), 2.35 (s, 18 Hz), 2.92 (t, 6H, *J* =7.8 Hz), 6.74 (d, 12H, *J* =8.2 Hz), 6.84 (d, 3H, *J* =3.8 Hz), 6.94 (d, 12H, *J* =8.2 Hz), 7.16 (s, 6H), 7.18 (d, 3H, *J* =4.3 Hz), 7.20 (d, 3H, *J* =3.8 Hz), 7.92 (d, 3H, *J* =4.3 Hz). ^{13}C NMR (125 MHz, $CDCl_3$): δ [ppm] 13.82, 20.87, 22.34, 29.11, 30.32, 31.23, 37.54, 55.44, 76.78, 113.77, 114.57, 123.59, 124.78, 125.48, 127.50, 127.99, 128.46, 129.73, 129.99, 133.62, 134.75, 134.87,

135.20, 135.90, 142.31, 146.73, 146.84, 166.23. Calcd (%) for $C_{117}H_{117}NS_6$: C, 81.25; H, 6.82; S, 11.12; N, 0.81. Found C, 81.35; H, 6.74; S, 11.12; N, 0.78.

2. ^{1}H and ^{13}C NMR Spectra

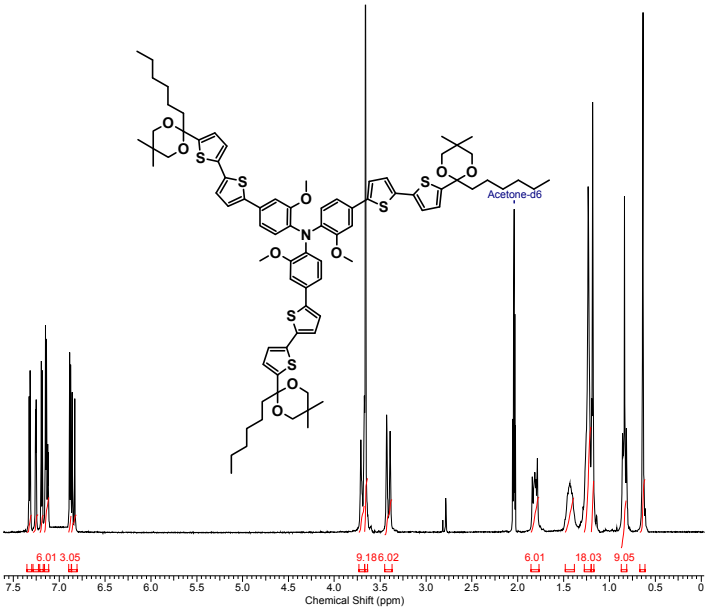

No.	Annotation	(ppm)
1	Acetone-d6	2.04

No.	(ppm)	Value	Absolute Value
1	[0.61 .. 0.67]	9.015	4.03353e+9
2	[0.81 .. 0.87]	9.054	4.05092e+9
3	[1.17 .. 1.20]	9.071	4.05867e+9
4	[1.20 .. 1.27]	18.034	8.06872e+9
5	[1.38 .. 1.48]	6.085	2.72241e+9
6	[1.77 .. 1.86]	6.015	2.69107e+9
7	[3.37 .. 3.45]	6.017	2.69196e+9
8	[3.64 .. 3.67]	9.184	4.10919e+9
9	[3.67 .. 3.73]	6.002	2.68536e+9
10	[6.81 .. 6.87]	2.996	1.34036e+9
11	[6.87 .. 6.90]	3.052	1.36571e+9
12	[7.11 .. 7.16]	6.007	2.68748e+9
13	[7.17 .. 7.21]	3.006	1.34510e+9
14	[7.23 .. 7.29]	3.007	1.34533e+9
15	[7.30 .. 7.35]	3.000	1.34232e+9

Figure S2.1. ^{1}H NMR spectrum of compound **3a** in Acetone-d6.

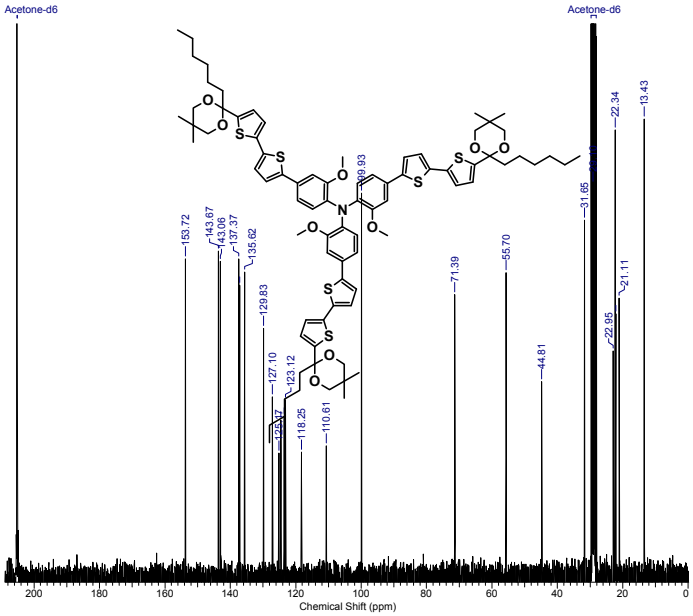

No.	(ppm)	(Hz)	Height
1	13.43	1013.4	0.1097
2	21.11	1593.4	0.0671
3	22.09	1667.4	0.0634
4	22.34	1686.5	0.1071
5	22.95	1732.4	0.0546
6	29.10	2196.3	0.0943
7	31.65	2389.2	0.0857
8	44.81	3382.1	0.0472
9	55.70	4204.0	0.0732
10	71.39	5388.2	0.0680
11	99.93	7542.7	0.0920
12	110.61	8348.8	0.0321
13	118.25	8925.4	0.0305

No.	(ppm)	(Hz)	Height
14	123.12	9292.8	0.0429
15	123.49	9320.7	0.0390
16	124.57	9402.3	0.0382
17	125.17	9447.3	0.0303
18	127.10	9593.3	0.0437
19	129.83	9799.5	0.0599
20	135.62	10236.0	0.0733
21	137.12	10349.3	0.0702
22	137.37	10368.4	0.0765
23	143.06	10797.7	0.0758
24	143.67	10844.1	0.0783
25	153.72	11602.4	0.0765

No.	Annotation	(ppm)
1	Acetone-d6	[28.11 .. 29.65]
2	Acetone-d6	205.17

Figure S2.2. ^{13}C NMR spectrum of compound **3a** in Acetone-d6.

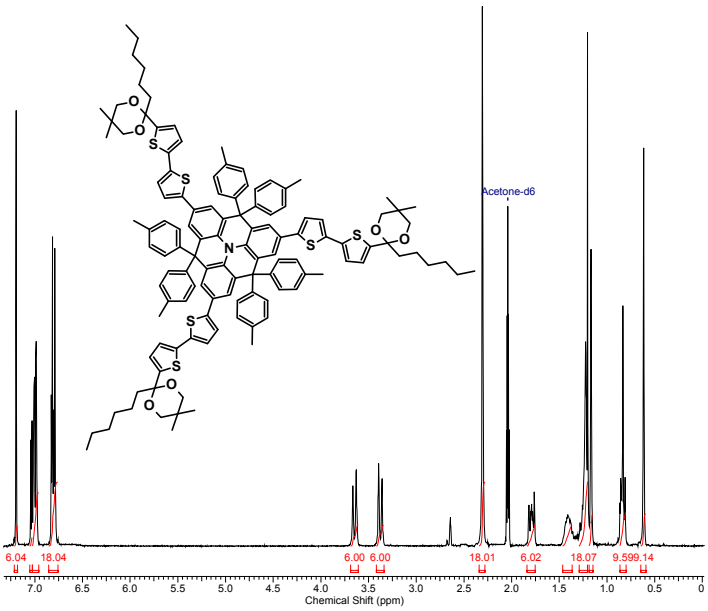

No.	Annotation	(ppm)
1	Acetone-d6	2.04

No.	(ppm)	Value	Absolute Value
1	[0.59 .. 0.64]	9.144	4.58026e+9
2	[0.80 .. 0.86]	9.592	4.80471e+9
3	[1.15 .. 1.19]	9.078	4.54698e+9
4	[1.21 .. 1.29]	18.071	9.05146e+9
5	[1.36 .. 1.46]	6.064	3.03752e+9
6	[1.76 .. 1.84]	6.015	3.01285e+9
7	[2.28 .. 2.34]	18.007	9.01955e+9
8	[3.34 .. 3.42]	6.002	3.00657e+9
9	[3.61 .. 3.69]	5.998	3.00449e+9
10	[6.76 .. 6.85]	18.044	9.03809e+9
11	[6.96 .. 7.03]	15.020	7.52342e+9
12	[7.03 .. 7.05]	3.083	1.54421e+9
13	[7.18 .. 7.22]	6.045	3.02766e+9

Figure S2.3. ^{1}H NMR spectrum of compound **3b** in Acetone-d6.

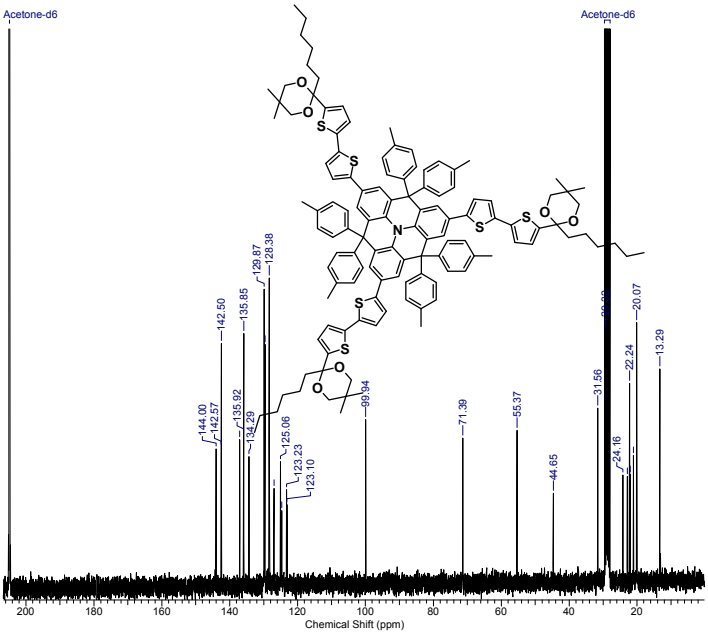

No.	(ppm)	(Hz)	Height
1	13.29	1003.2	0.0545
2	20.07	1514.6	0.0662
3	21.06	1589.8	0.0327
4	22.04	1663.3	0.0280
5	22.24	1678.5	0.0509
6	22.86	1725.8	0.0275
7	24.16	1823.6	0.0279
8	29.32	2213.1	0.0644
9	31.56	2381.7	0.0447
10	44.65	3370.0	0.0233
11	55.37	4179.1	0.0392
12	71.39	5388.2	0.0372
13	99.94	7543.0	0.0418
14	123.10	9291.1	0.0205
15	123.23	9301.1	0.0242

No.	(ppm)	(Hz)	Height
16	124.62	9406.4	0.0189
17	125.06	9439.0	0.0312
18	126.97	9583.3	0.0246
19	128.38	9690.0	0.0773
20	128.44	9694.2	0.0392
21	129.60	9782.1	0.0607
22	129.87	9802.3	0.0745
23	134.29	10135.6	0.0325
24	135.85	10253.4	0.0634
25	135.92	10258.9	0.0381
26	137.04	10343.5	0.0368
27	142.50	10755.4	0.0609
28	142.57	10760.9	0.0349
29	144.00	10869.0	0.0344

No.	Annotation	(ppm)
1	Acetone-d6	[28.00 .. 29.55]
2	Acetone-d6	[204.89 .. 204.90]

Figure S2.4. ^{13}C NMR spectrum of compound **3b** in Acetone-d6.

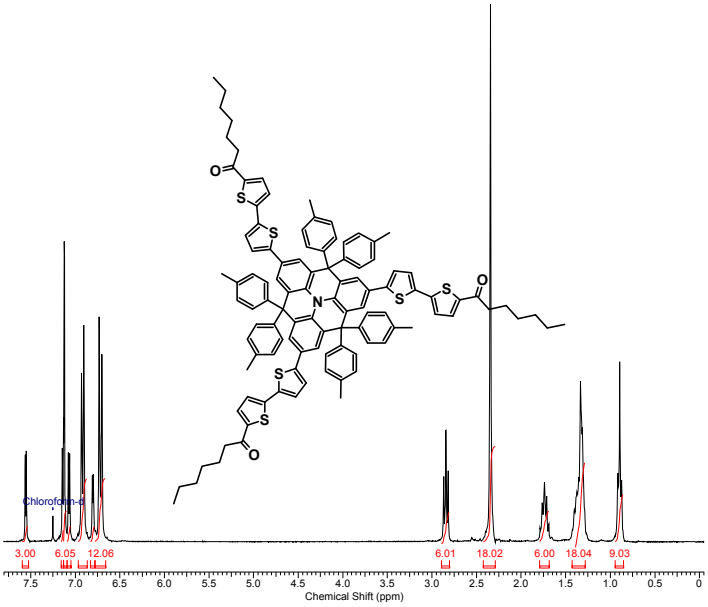

No.	Annotation	(ppm)
1	Chloroform-d	7.25

No.	(ppm)	Value	Absolute Value
1	[0.85 .. 0.94]	9.030	5.60462e+9
2	[1.28 .. 1.43]	18.037	1.11947e+10
3	[1.68 .. 1.79]	6.003	3.72584e+9
4	[2.29 .. 2.42]	18.017	1.11827e+10
5	[2.80 .. 2.89]	6.008	3.72866e+9
6	[6.66 .. 6.78]	12.061	7.48607e+9
7	[6.78 .. 6.83]	3.001	1.86269e+9
8	[6.87 .. 6.97]	12.036	7.47029e+9
9	[7.05 .. 7.09]	2.998	1.86060e+9
10	[7.09 .. 7.13]	6.046	3.75252e+9
11	[7.13 .. 7.16]	3.012	1.86952e+9
12	[7.53 .. 7.59]	3.000	1.86199e+9

Figure S2.5. ^{1}H NMR spectrum of compound **4a** in $CDCl_3$.

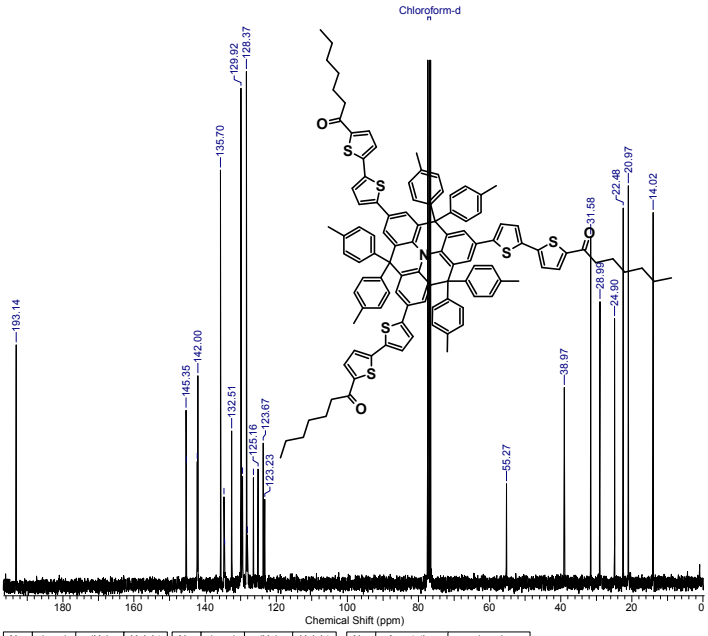

No.	(ppm)	(Hz)	Height
1	14.02	1058.2	0.5463
2	20.97	1582.9	0.5854
3	22.48	1696.5	0.5530
4	24.90	1879.5	0.3906
5	28.99	2188.2	0.4157
6	31.58	2383.4	0.5108
7	38.97	2941.2	0.2900
8	55.27	4171.9	0.1487
9	123.23	9301.4	0.1258
10	123.67	9334.5	0.2086
11	125.16	9446.5	0.1705
12	126.42	9541.9	0.1577
13	128.08	9667.1	0.0732

No.	(ppm)	(Hz)	Height
14	128.37	9689.2	0.7528
15	129.49	9773.8	0.1594
16	129.92	9806.4	0.7285
17	132.51	10001.6	0.2263
18	134.52	10153.6	0.0556
19	134.70	10167.2	0.1294
20	135.70	10242.6	0.6083
21	142.00	10717.8	0.3070
22	142.20	10732.7	0.1813
23	145.30	10966.9	0.1760
24	145.35	10970.7	0.2565
25	193.14	14577.9	0.3524

No.	Annotation	(ppm)
1	Chloroform-d	[76.57 .. 77.43]

Figure S2.6. ^{13}C NMR spectrum of compound **4a** in $CDCl_3$.

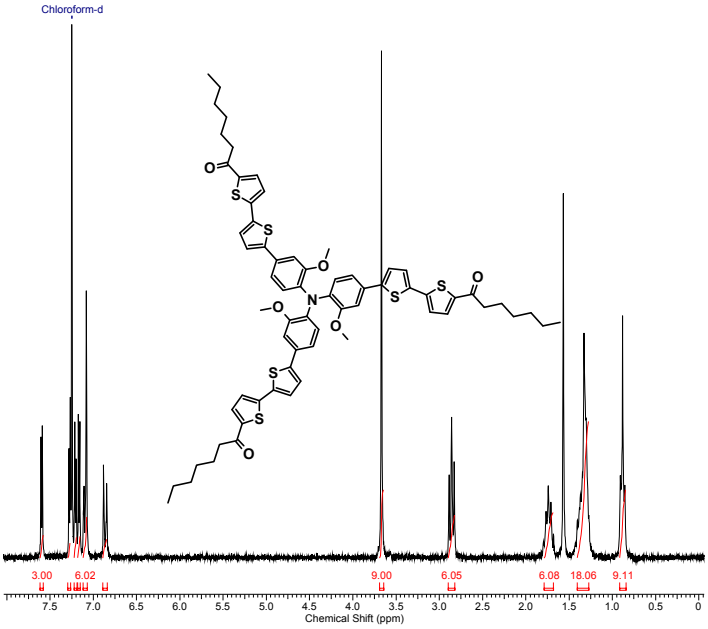

No.	Annotation	(ppm)
1	Chloroform-d	7.25

No.	(ppm)	Value	Absolute Value
1	[0.84 .. 0.92]	9.111	2.25740e+7
2	[1.27 .. 1.41]	18.058	4.47405e+7
3	[1.68 .. 1.79]	6.076	1.50543e+7
4	[2.82 .. 2.90]	6.054	1.50001e+7
5	[3.64 .. 3.69]	9.000	2.22979e+7
6	[6.84 .. 6.89]	3.010	7.45636e+6
7	[7.07 .. 7.12]	6.016	1.49053e+7
8	[7.15 .. 7.18]	3.071	7.60791e+6
9	[7.19 .. 7.22]	3.064	7.59106e+6
10	[7.26 .. 7.30]	3.048	7.55249e+6
11	[7.58 .. 7.61]	3.002	7.43666e+6

Figure S2.7. ^{1}H NMR spectrum of compound **4b** in $CDCl_3$.

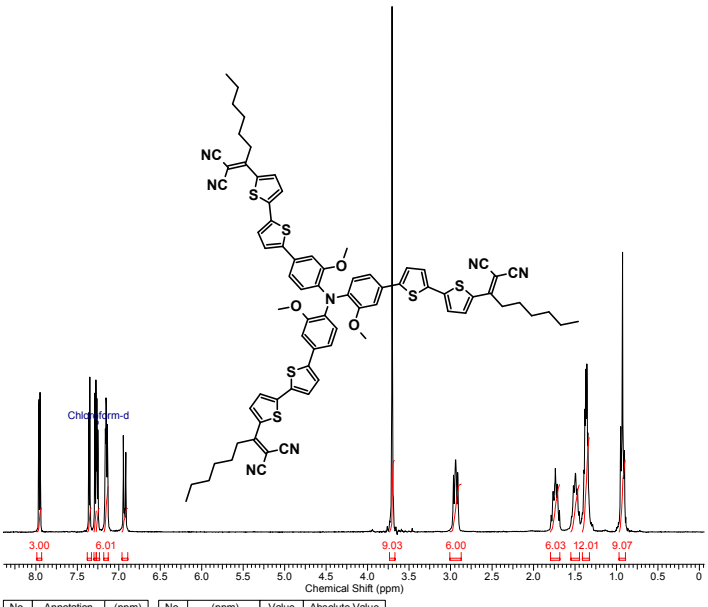

No.	Annotation	(ppm)
1	Chloroform-d	7.25

No.	(ppm)	Value	Absolute Value
1	[0.89 .. 0.97]	9.073	6.58244e+9
2	[1.32 .. 1.41]	12.009	8.71289e+9
3	[1.45 .. 1.55]	6.003	4.35493e+9
4	[1.68 .. 1.79]	6.028	4.37327e+9
5	[2.87 .. 3.01]	5.998	4.35142e+9
6	[3.67 .. 3.74]	9.029	6.55085e+9
7	[6.89 .. 6.96]	3.018	2.18971e+9
8	[7.13 .. 7.18]	6.007	4.35850e+9
9	[7.23 .. 7.27]	2.982	2.16331e+9
10	[7.27 .. 7.30]	3.035	2.20215e+9
11	[7.33 .. 7.38]	3.013	2.18619e+9
12	[7.93 .. 7.99]	3.000	2.17654e+9

Figure S2.8. ^{1}H NMR spectrum of compound **m-TPA** in $CDCl_3$.

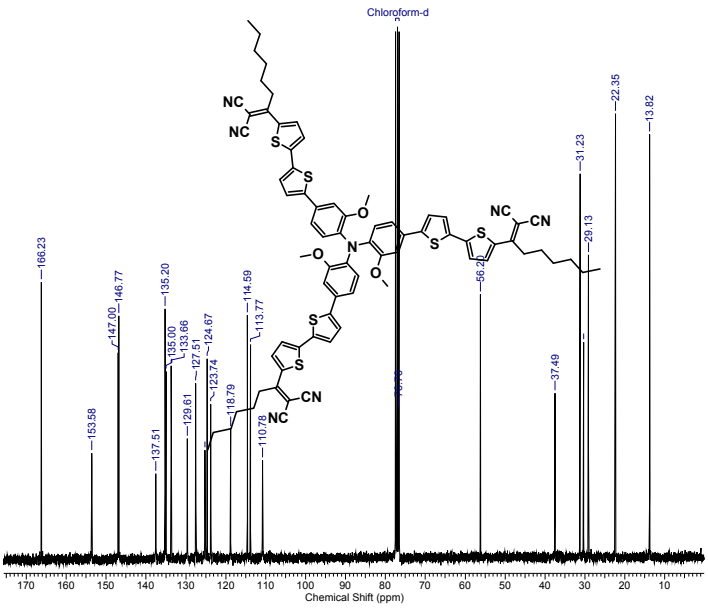

No.	(ppm)	(Hz)	Height
1	13.82	1043.2	0.7987
2	22.35	1686.8	0.8373
3	29.13	2198.7	0.5734
4	30.36	2291.3	0.4102
5	31.23	2357.4	0.7254
6	37.49	2829.5	0.3146
7	56.20	4241.5	0.4994
8	76.76	5793.4	0.2839
9	110.78	8361.5	0.1892
10	113.77	8587.3	0.4055
11	114.59	8649.2	0.4608
12	118.79	8966.3	0.2475
13	123.74	9339.8	0.2940

No.	(ppm)	(Hz)	Height
14	124.67	9409.7	0.3790
15	125.18	9448.7	0.2077
16	127.51	9624.2	0.3329
17	129.61	9782.6	0.2292
18	133.66	10088.3	0.3658
19	135.00	10189.5	0.3552
20	135.20	10204.4	0.4725
21	137.51	10378.9	0.1637
22	146.77	11078.2	0.4591
23	147.00	11095.1	0.3903
24	153.58	11591.6	0.2027
25	166.23	12546.6	0.5224

No.	Annotation	(ppm)
1	Chloroform-d	[76.60 .. 77.41]

Figure S2.9. ^{13}C NMR spectrum of compound **m-TPA** in $CDCl_3$.

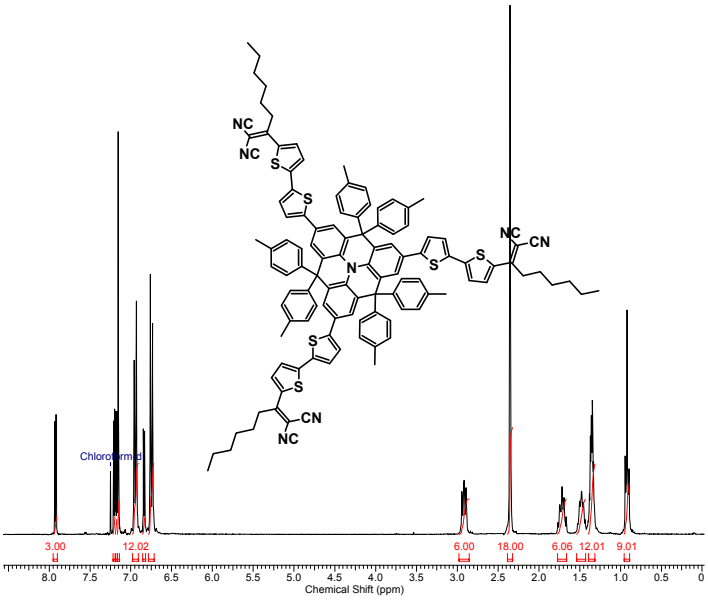

No.	Annotation	(ppm)
1	Chloroform-d	7.25

No.	(ppm)	Value	Absolute Value
1	[0.89 .. 0.96]	9.010	4.47712e+9
2	[1.31 .. 1.39]	12.013	5.96916e+9
3	[1.43 .. 1.54]	6.030	2.99623e+9
4	[1.66 .. 1.77]	6.058	3.01024e+9
5	[2.32 .. 2.38]	18.004	8.94574e+9
6	[2.86 .. 2.98]	5.996	2.97911e+9
7	[6.71 .. 6.79]	12.010	5.96753e+9
8	[6.82 .. 6.86]	3.006	1.49382e+9
9	[6.91 .. 6.98]	12.022	5.97355e+9
10	[7.14 .. 7.16]	6.017	2.98982e+9
11	[7.17 .. 7.19]	3.018	1.49949e+9
12	[7.19 .. 7.22]	3.013	1.49711e+9
13	[7.90 .. 7.95]	3.000	1.49068e+9

Figure S2.10. ^{1}H NMR spectrum of compound **f-TPA** in $CDCl_3$.

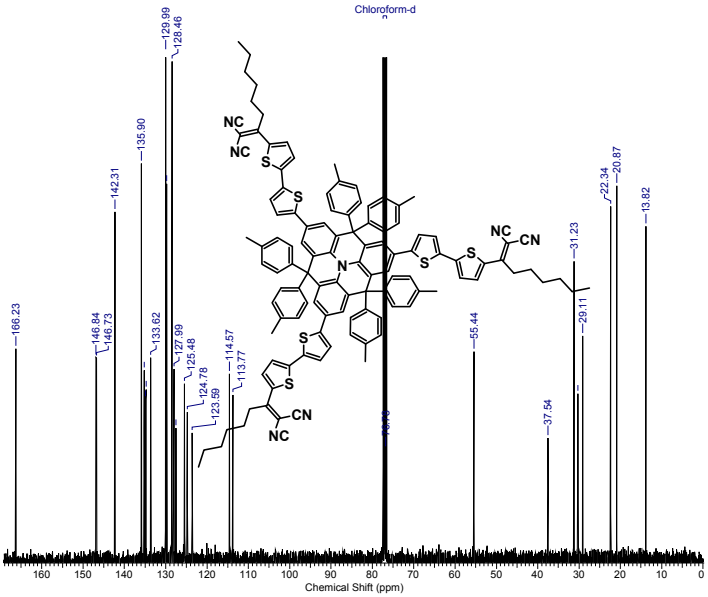

No.	(ppm)	(Hz)	Height
1	13.82	1043.2	0.6278
2	20.87	1575.4	0.7026
3	22.34	1686.2	0.6643
4	29.11	2197.1	0.4258
5	30.32	2288.3	0.3196
6	31.23	2357.1	0.5635
7	37.54	2833.4	0.2381
8	55.44	4184.3	0.3970
9	76.78	5794.8	0.2170
10	113.77	8587.3	0.3174
11	114.57	8647.3	0.3558
12	123.59	9328.2	0.2472
13	124.78	9418.3	0.2853
14	125.48	9471.1	0.3376

No.	(ppm)	(Hz)	Height
15	127.50	9623.4	0.2563
16	127.99	9660.7	0.3649
17	128.46	9695.8	0.9321
18	129.73	9792.0	0.7064
19	129.99	9811.1	0.9407
20	133.62	10085.0	0.3858
21	134.75	10171.0	0.3274
22	134.87	10179.6	0.3095
23	135.20	10204.4	0.3622
24	135.90	10257.2	0.7438
25	142.31	10741.0	0.6543
26	146.73	11075.2	0.3846
27	146.84	11082.9	0.3865
28	166.23	12546.6	0.4024

No.	Annotation	(ppm)
1	Chloroform-d	[76.55 .. 77.40]

Figure S2.11. ^{13}C NMR spectrum of compound **f-TPA** in $CDCl_3$.

3. Charge transport and photovoltaic properties

3.1. Solar cells fabrication and characterization

The samples of organic solar cells were prepared in the following way. First, glass substrates coated with patterned indium-tin oxide (ITO) layer (Xin Yan Technology Limited) were cleaned in an ultrasonic bath with a surfactant and isopropanol and then exposed to an ultraviolet lamp (Photo Surface Processor PL16-110, Sen Lights Corporation, 15 mW/cm^2, 254 nm). Then a 50-nm-thick layer of poly(ethylenedioxythiophene):polystyrene sulfonate (PEDOT:PSS, CLEVIOS P VP AI 4083, Heraeus GmbH, Germany) was deposited on the ITO by spin coating at 3000 rpm and annealed at 140 °C for 15 minutes. The active layer was deposited on the PEDOT:PSS layer by doctor blading from chloroform solution with a concentration of 11 g/L, at 50°C (the resulting thickness was 55±5 nm) for single component cells or from orthodichlorobenzene solution with a concentration of 24 g/L, 90°C (the resulting thickness was 85±5 nm) for BHJ cells. On top of the active layer Ca (20 nm) / Al (80 nm) electrode was evaporated under pressure less than $5 \cdot 10^{-6}$ mbar with the use of a vacuum evaporator (Univex 300, Leybold) integrated in a glove box with Ar atmosphere (H_2O < 0.1 ppm, O_2 < 5 ppm). Eight devices with the active area of each device 3 mm^2 were formed on substrates by using a shadow mask.

All the electrical measurements were performed in a glove box with Ar atmosphere (H_2O < 0.1 ppm, O_2 < 5 ppm). *J-V* characteristics of cells were measured using a source-meter (SourceMeter 2400, Keithley) in dark and under light of a solar simulator (Newport 67005) with an intensity of 100 mW/cm^2 (AM1.5G).

External quantum efficiency (EQE) spectra were measured with the use of a laser-driven light source (LDLS EQ-99X, Energetiq) equipped by a monochromator (CS130-USB-3-MC, Newport), a power sensor (S120UV, Thorlabs) and source-meter (SourceMeter 2400, Keithley). To avoid higher diffraction orders, additional filters KG3, GG400, OG550 (Newport) were used for 380-500, 480-620 and 600-800 nm spectral ranges respectively.

To study the surface morphology of the active layer, an atomic force microscope (AFM) (SOLVER NEXT, NT-MDT) operating in the semi-contact mode was used. Probes (HA_FM ETALON, NT-MDT) with the tip radius of curvature of 10 nm, the resonant frequencies of 77 – 114 kHz and force constant of 3.5 – 6 N/m were used.

3.2. Mobility measurements

Charge-carrier mobility were determined from space charge limited current (SCLC) measurements on unipolar thin-film devices of several thicknesses. Unipolar devices were made similarly to solar cells. The structure of the hole-only devices was ITO/PEDOT:PSS/active layer/Ag. The structure of the electron-only devices was ITO/ZnO/active layer/Ca. The ZnO layer was deposited on the ITO layer in the following way. First, 100 mg of zinc acetate dihydrate were dissolved in a mixture of 1 mL of 2-methoxyethanol and 27 μL of monoethanolamine. Then, this solution was bladed on the ITO layer and annealed at 140 °C for 25 minutes, resulting in a 40 nm-ZnO layer. Eight devices were formed on one substrate. The hole and electron mobilities were extracted by fitting the current–voltage (*J-V*) characteristics of the corresponding devices with the simplest SCLC model.

According to the simplest SCLC model and taking into account the series (R_s) and shunt (R_{sh}) resistances (as fitting parameters), the charge mobility was calculated by approximating the dark *J-V* curves of unipolar devices using the following equation:

$$J = \frac{9}{8}\varepsilon\varepsilon_0\mu\frac{(V - V_{BI} - JSR_s)^2}{d^3} + \frac{V - JSR_s}{R_{sh}},$$

where $\varepsilon_0 = 8.85 \cdot 10^{-12}$ F/m, ε is the dielectric permittivity (taken as 3), d is the active layer thickness (measured by AFM), V_{BI} is the built-in voltage (fitting parameter).

3.3. Hole mobility in pristine films

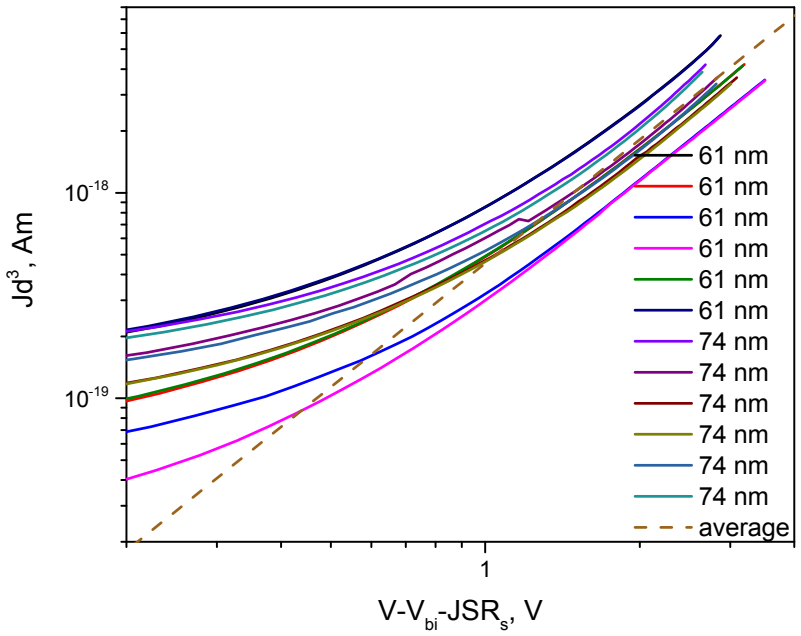

Figure S3.1. *J-V* characteristics of **TPA** hole only devices (solid lines). Jd^3 is plotted for two different layer thicknesses (61±5 and 74±5 nm) against the voltage, corrected for the built-in voltage and the electrode series resistance. Dashed line represents SCLC-fit, from which the hole mobility is extracted.

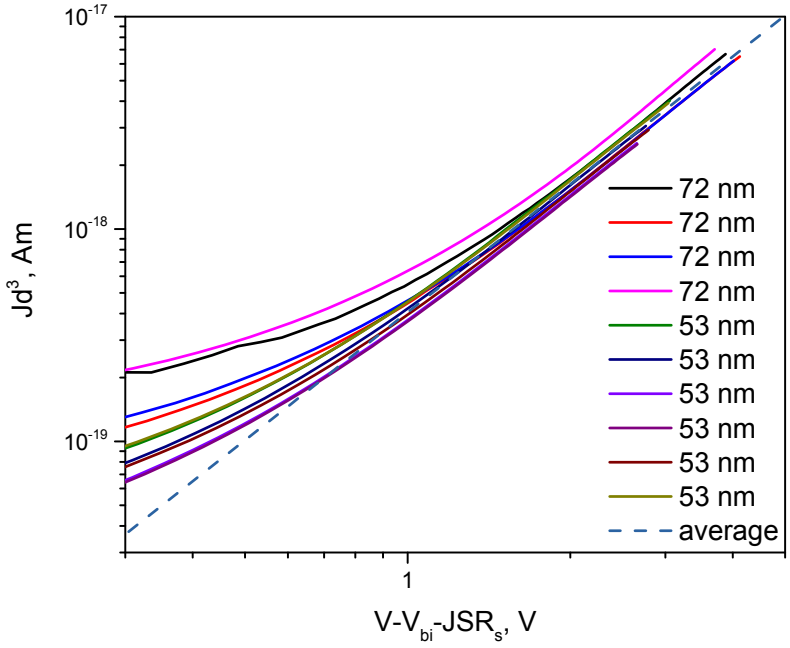

Figure S3.2. *J-V* characteristics of **m-TPA** hole only devices (solid lines). Jd^3 is plotted for two different layer thicknesses (53±5 and 72±5 nm) against the voltage, corrected for the built-in voltage and the electrode series resistance. Dashed line represents SCLC-fit, from which the hole mobility is extracted.

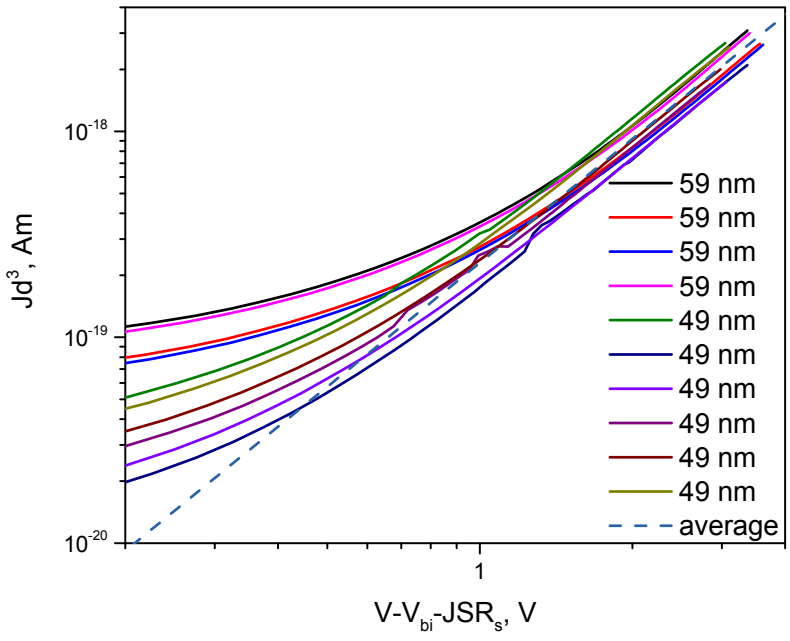

Figure S3.3. *J-V* characteristics of **f-TPA** hole only devices (solid lines). Jd^3 is plotted for two different layer thicknesses (49±5 and 59±5 nm) against the voltage, corrected for the built-in

voltage and the electrode series resistance. Dashed line represents SCLC-fit, from which the hole mobility is extracted.

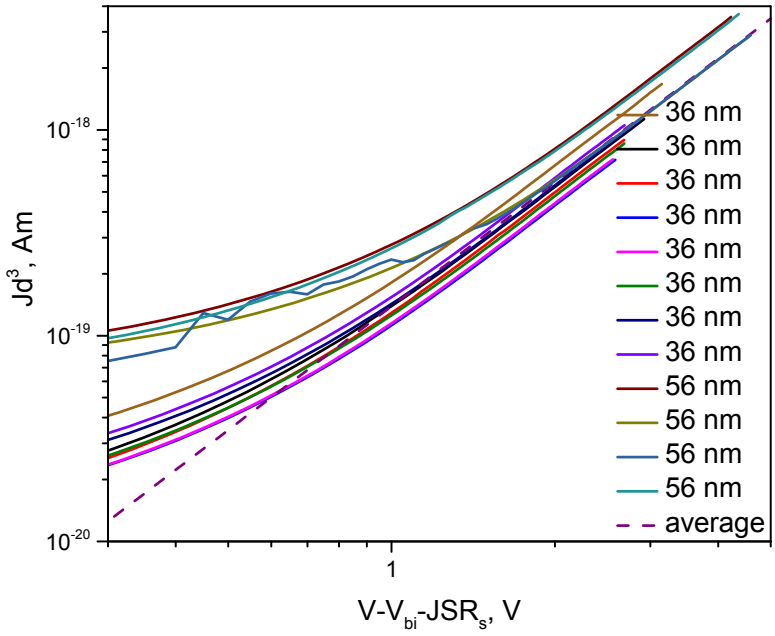

Figure S3.4. *J-V* characteristics of **s-CBZ** hole only devices (solid lines). Jd^3 is plotted for two different layer thicknesses (36±5 and 56±5 nm) against the voltage, corrected for the built-in voltage and the electrode series resistance. Dashed line represents SCLC-fit, from which the hole mobility is extracted.

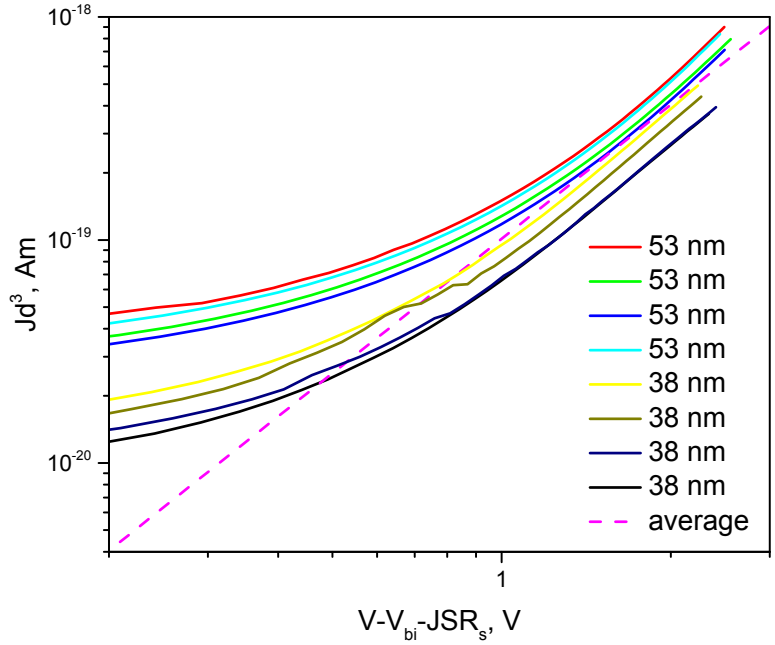

Figure S3.5. *J-V* characteristics of **t-CBZ** hole only devices (solid lines). Jd^3 is plotted for two different layer thicknesses (38±5 and 53±5 nm) against the voltage, corrected for the built-in voltage and the electrode series resistance. Dashed line represents SCLC-fit, from which the hole mobility is extracted.

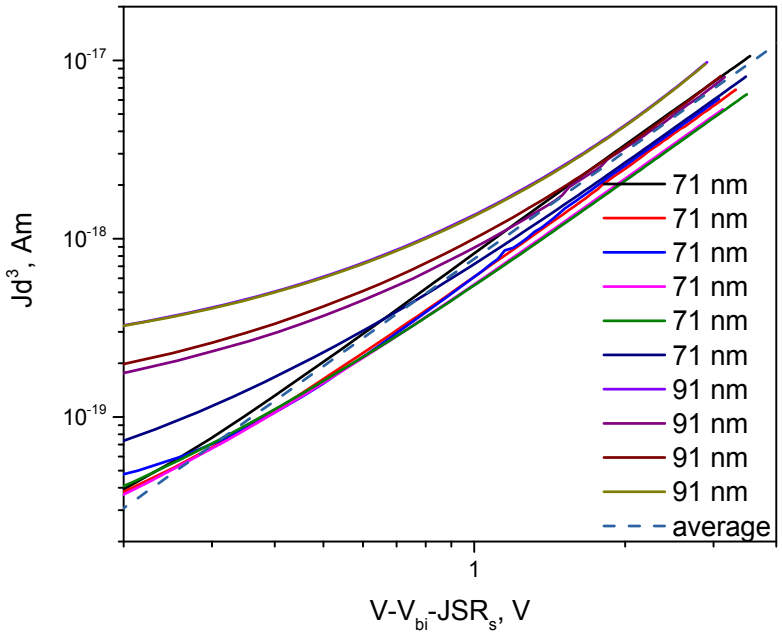

Figure S3.6. *J-V* characteristics of **BTI** hole only devices (solid lines). Jd^3 is plotted for two different layer thicknesses (71±5 and 91±5 nm) against the voltage, corrected for the built-in voltage and the electrode series resistance. Dashed line represents SCLC-fit, from which the hole mobility is extracted.

3.4. Electron mobility in pristine films

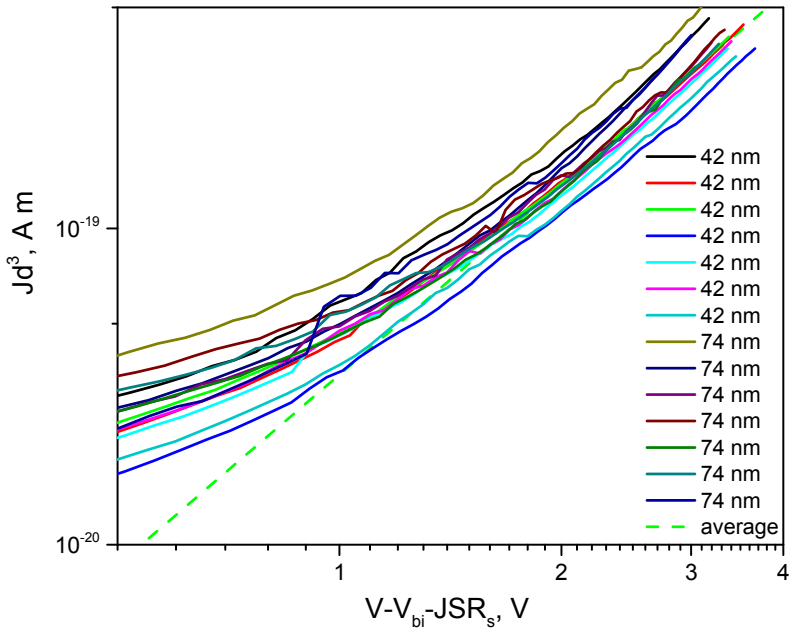

Figure S3.7. *J-V* characteristics of **TPA** electron only devices (solid lines). Jd^3 is plotted for two different layer thicknesses (42±5 and 74±5 nm) against the voltage, corrected for the built-in

voltage and the electrode series resistance. Dashed line represents SCLC-fit, from which the electron mobility is extracted.

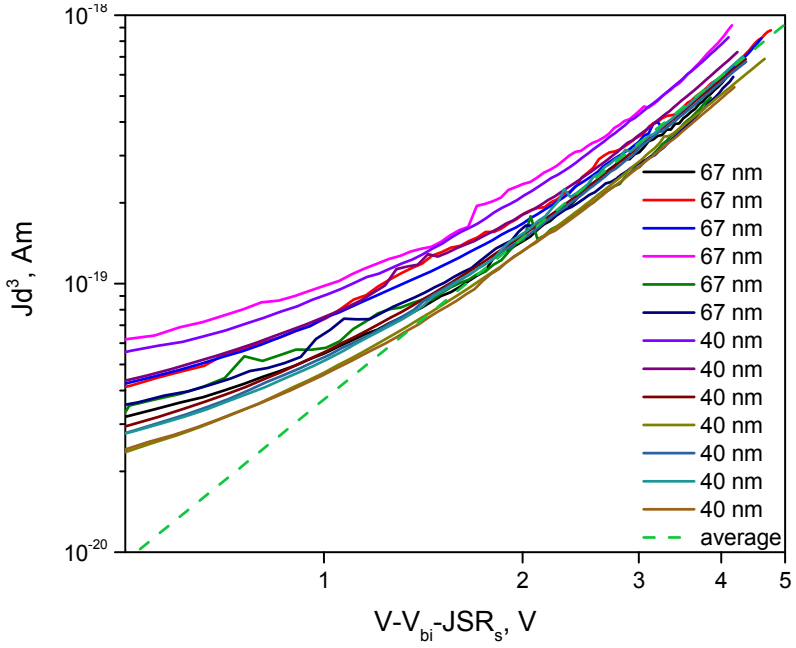

Figure S3.8. *J-V* characteristics of **m-TPA** electron only devices (solid lines). Jd^3 is plotted for two different layer thicknesses (40±5 and 67±5 nm) against the voltage, corrected for the built-in voltage and the electrode series resistance. Dashed line represents SCLC-fit, from which the electron mobility is extracted.

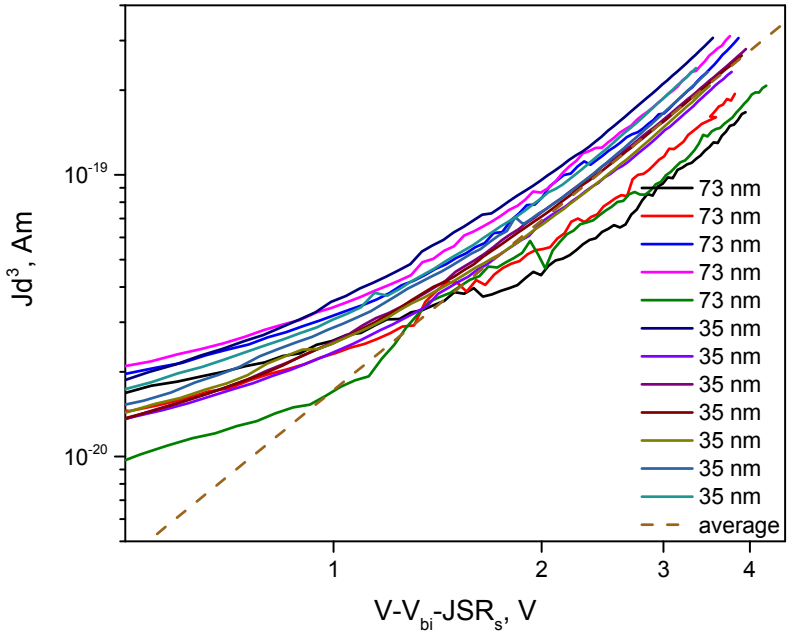

Figure S3.9. *J-V* characteristics of **f-TPA** electron only devices (solid lines). Jd^3 is plotted for two different layer thicknesses (35±5 and 73±5 nm) against the voltage, corrected for the built-in voltage and the electrode series resistance. Dashed line represents SCLC-fit, from which the electron mobility is extracted.

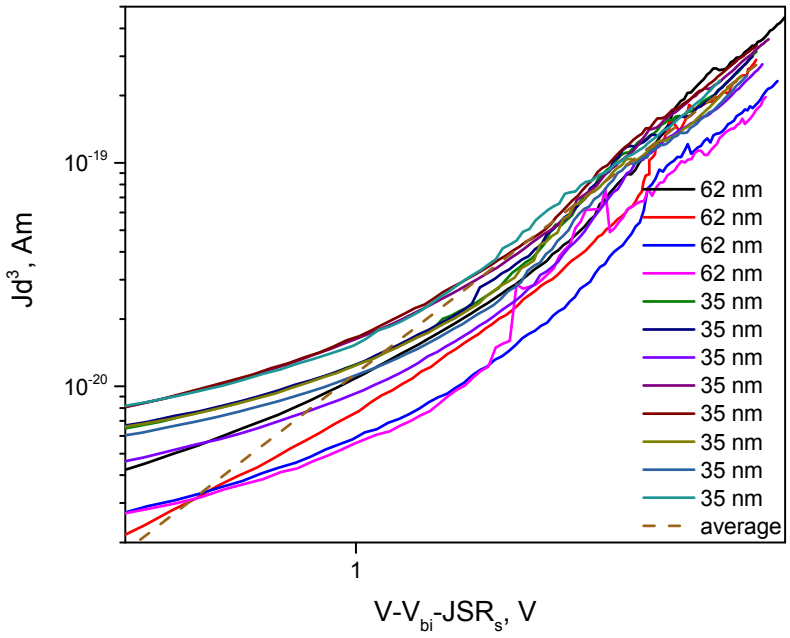

Figure S3.10. *J-V* characteristics of **s-CBZ** electron only devices (solid lines). Jd^3 is plotted for two different layer thicknesses (35±5 and 62±5 nm) against the voltage, corrected for the built-in voltage and the electrode series resistance. Dashed line represents SCLC-fit, from which the electron mobility is extracted.

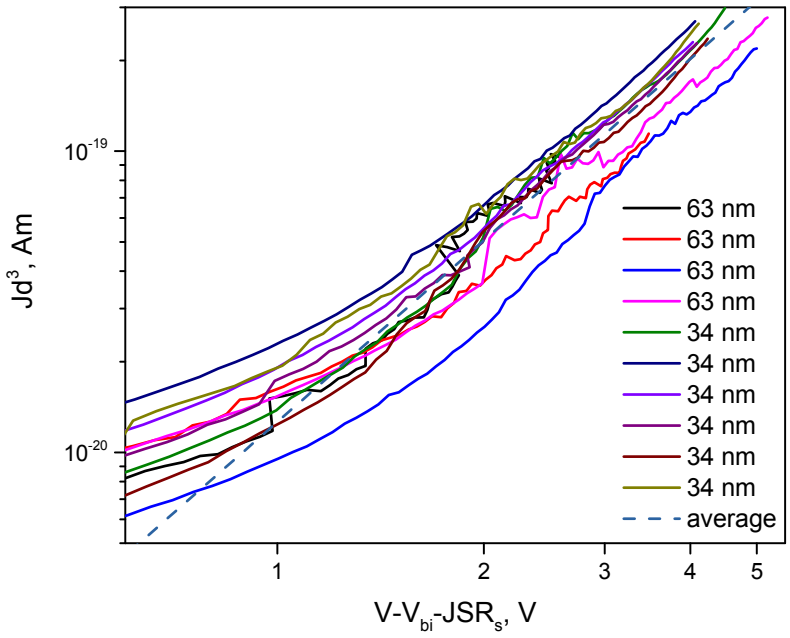

Figure S3.11. *J-V* characteristics of **t-CBZ** electron only devices (solid lines). Jd^3 is plotted for two different layer thicknesses (34±5 and 63±5 nm) against the voltage, corrected for the built-in

voltage and the electrode series resistance. Dashed line represents SCLC-fit, from which the electron mobility is extracted.

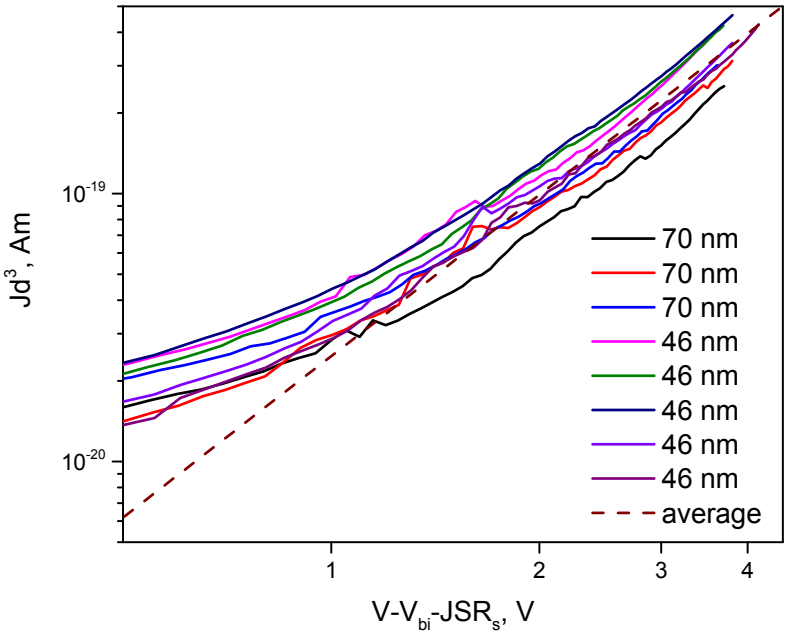

Figure S3.12. *J-V* characteristics of **BTI** electron only devices (solid lines). Jd^3 is plotted for two different layer thicknesses (46±5 and 70±5 nm) against the voltage, corrected for the built-in voltage and the electrode series resistance. Dashed line represents SCLC-fit, from which the electron mobility is extracted.

3.5. Hole mobility in blended films

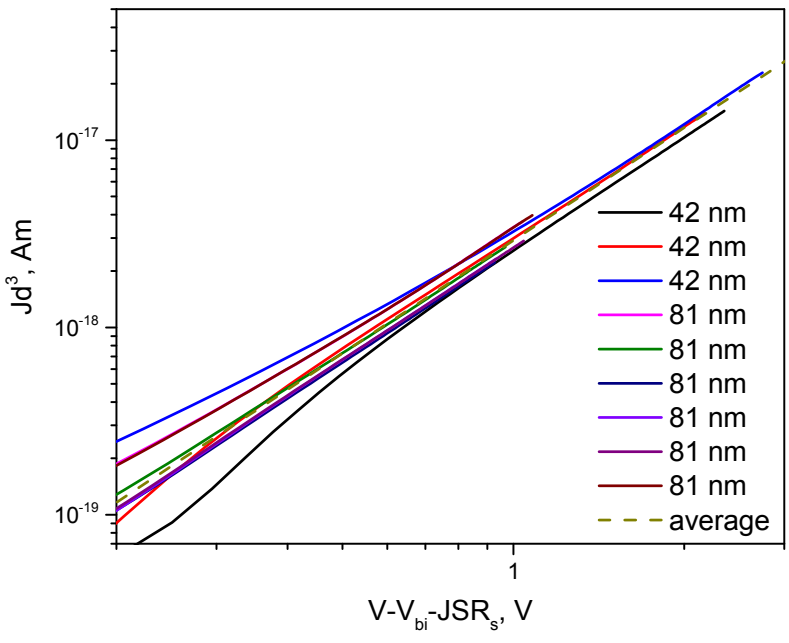

Figure S3.13. *J-V* characteristics of **TPA:PC$_{71}$BM** hole only devices (solid lines). Jd^3 is plotted for two different layer thicknesses (42±5 and 81±5 nm) against the voltage, corrected for the built-in voltage and the electrode series resistance. Dashed line represents SCLC-fit, from which the hole mobility is extracted.

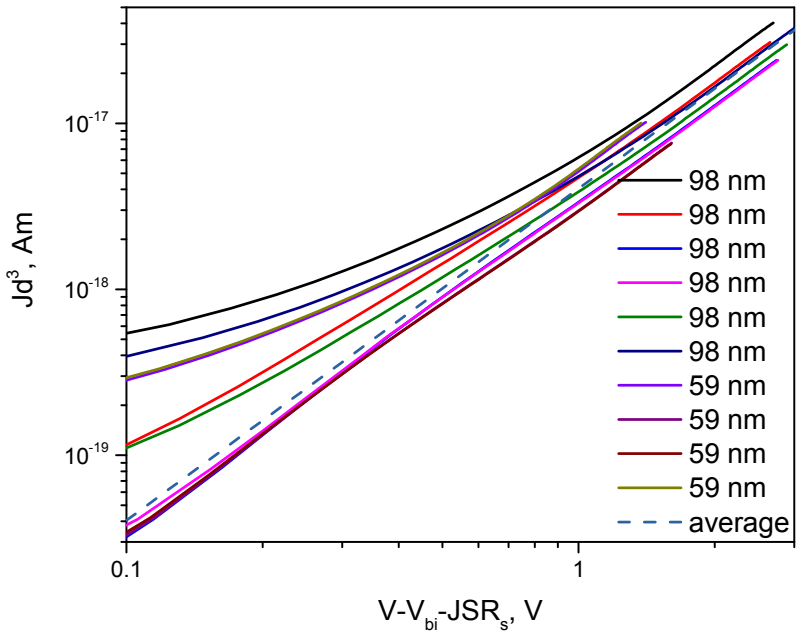

Figure S3.14. *J-V* characteristics of **m-TPA:PC$_{71}$BM** hole only devices (solid lines). Jd^3 is plotted for two different layer thicknesses (59±5 and 98±5 nm) against the voltage, corrected for the built-in voltage and the electrode series resistance. Dashed line represents SCLC-fit, from which the hole mobility is extracted.

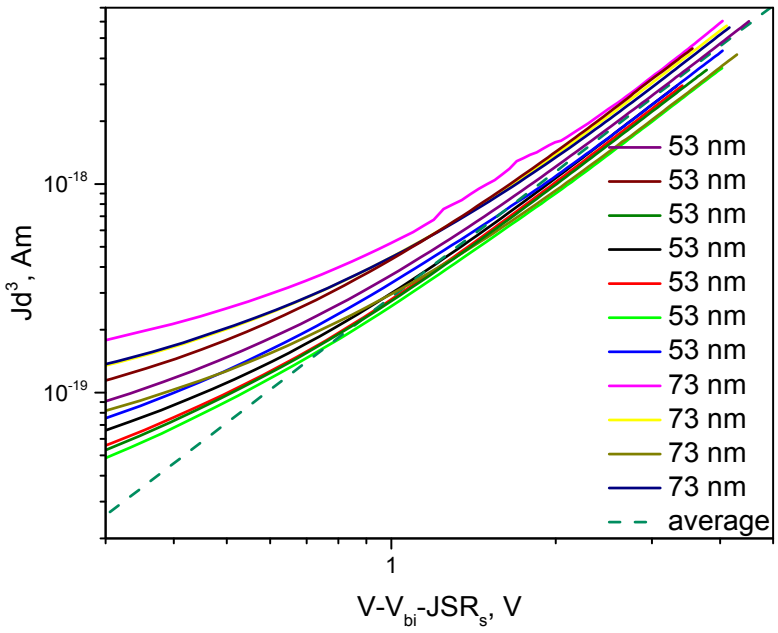

Figure S3.15. *J-V* characteristics of **f-TPA:PC$_{71}$BM** hole only devices (solid lines). Jd^3 is plotted for two different layer thicknesses (53±5 and 73±5 nm) against the voltage, corrected for the built-in voltage and the electrode series resistance. Dashed line represents SCLC-fit, from which the hole mobility is extracted.

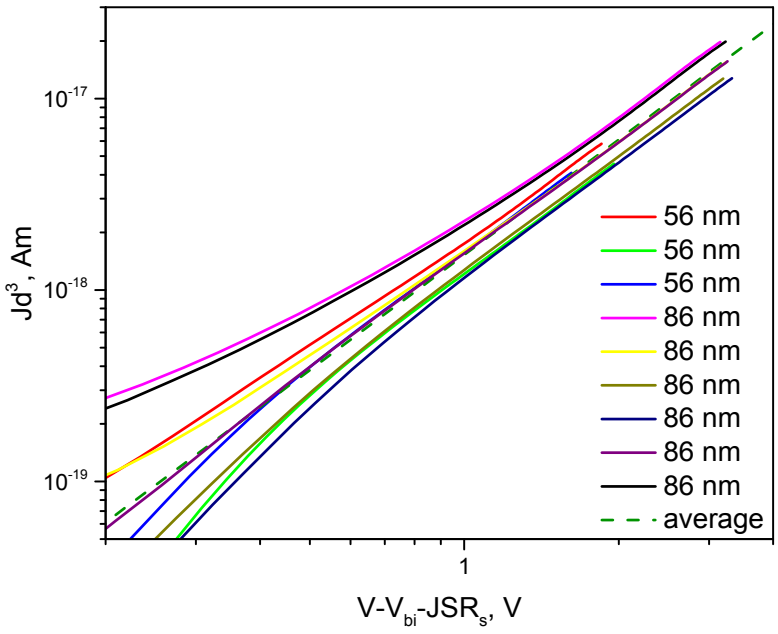

Figure S3.16. *J-V* characteristics of **s-CBZ:PC$_{71}$BM** hole only devices (solid lines). Jd^3 is plotted for two different layer thicknesses (56±5 and 86±5 nm) against the voltage, corrected for the built-in voltage and the electrode series resistance. Dashed line represents SCLC-fit, from which the hole mobility is extracted.

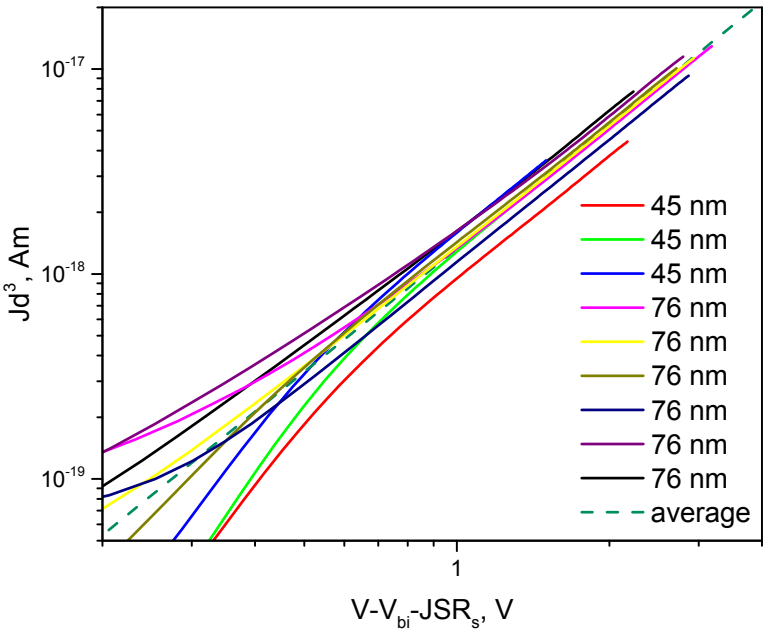

Figure S3.17. *J-V* characteristics of **t-CBZ:PC$_{71}$BM** hole only devices (solid lines). Jd^3 is plotted for two different layer thicknesses (45±5 and 76±5 nm) against the voltage, corrected for the built-in voltage and the electrode series resistance. Dashed line represents SCLC-fit, from which the hole mobility is extracted.

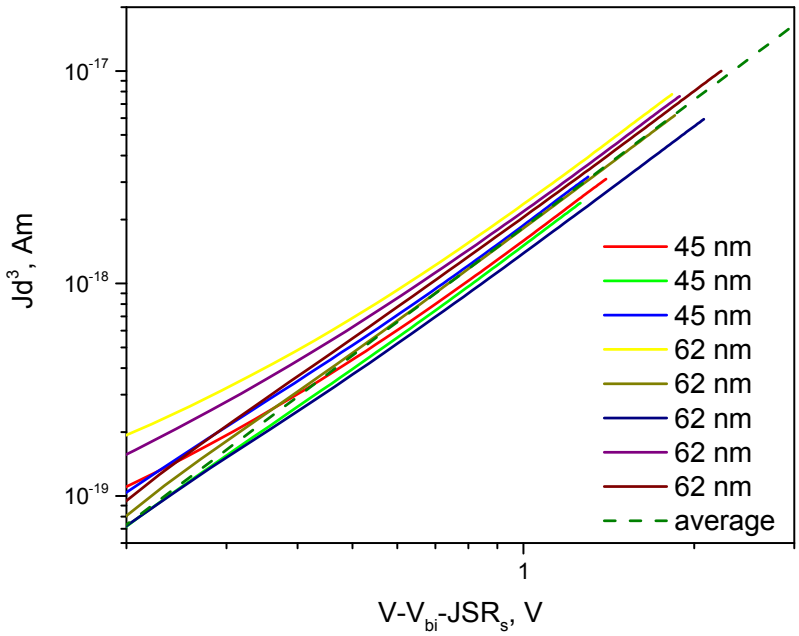

Figure S3.18. *J-V* characteristics of **BTI:PC$_{71}$BM** hole only devices (solid lines). Jd^3 is plotted for two different layer thicknesses (45±5 and 62±5 nm) against the voltage, corrected for the built-in voltage and the electrode series resistance. Dashed line represents SCLC-fit, from which the hole mobility is extracted.

3.6. Surface morphology of pristine films

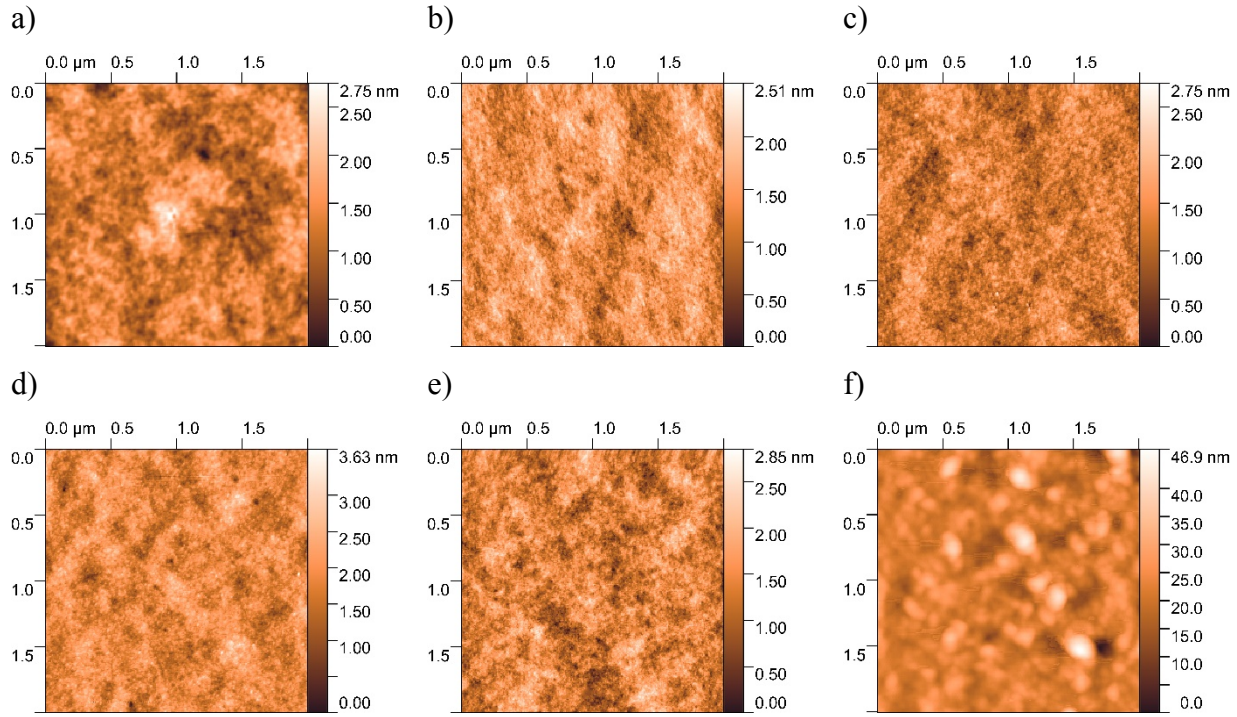

Figure S3.19. AFM surface scans of films of **TPA**, RMS=0.33 nm (a); **m-TPA**, RMS=0.31 nm (b); **f-TPA**, RMS=0.30 nm (c); **s-CBZ**, RMS=0.36 nm (d); **t-CBZ**, RMS=0.37 nm (e); **BTI**, RMS=4.60 nm (f).

3.7. Surface morphology of blended films

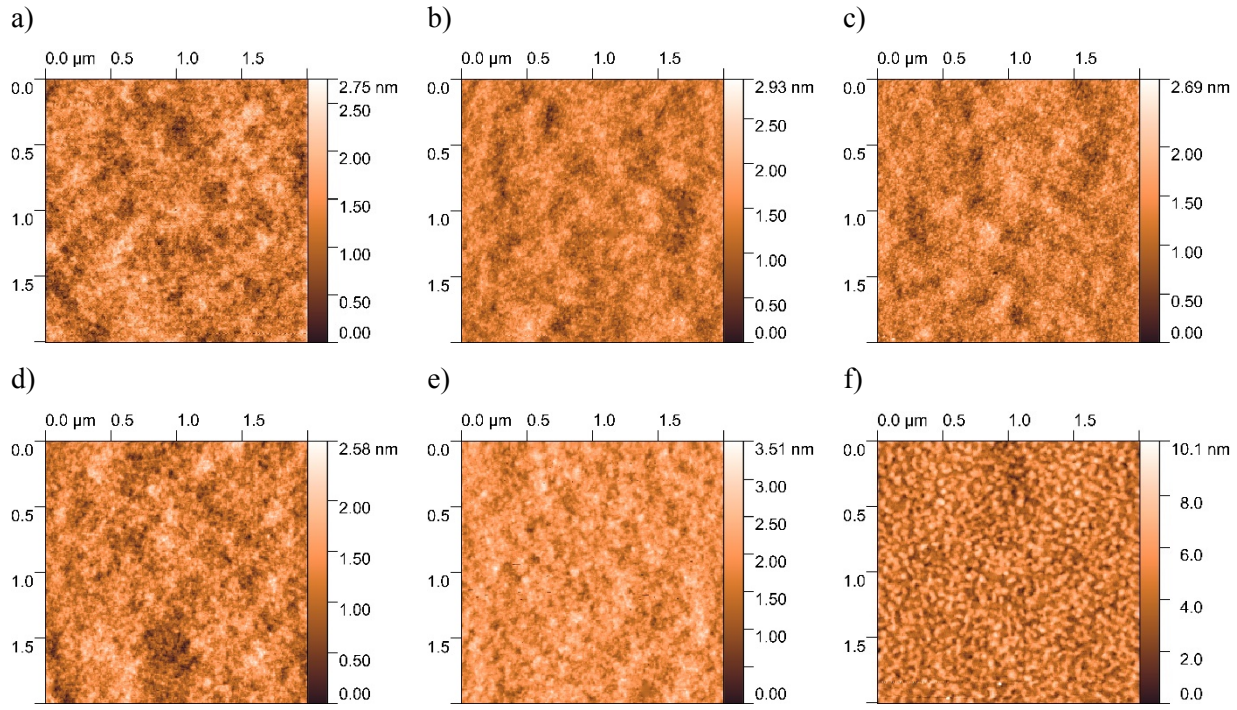

Figure S3.20. AFM surface scans of films of **TPA:PC$_{71}$BM**, RMS=0.36 nm (a); **m-TPA:PC$_{71}$BM**, RMS=0.30 nm (b); **f-TPA:PC$_{71}$BM**, RMS=0.31 nm (c); **s-CBZ:PC$_{71}$BM**, RMS=0.33 nm (d); **t-CBZ:PC$_{71}$BM**, RMS=0.36 nm (e); **BTI:PC$_{71}$BM**, RMS=1.28 nm (f).

3.7. Averaged photovoltaic parameters

Table S1. Photovoltaic parameters of SCOSCs under AM1.5G illumination (100 mW/cm^2) averaged over eight devices.

Active layer material	J_{SC}, mA/cm^2	V_{OC}, V	FF, %	PCE, %
TPA	1.66 ± 0.05	1.06 ± 0.13	24.7 ± 1.1	0.43 ± 0.04
m-TPA	1.628 ± 0.018	0.96 ± 0.14	24.6 ± 1.0	0.38 ± 0.04
f-TPA	0.524 ± 0.008	0.57 ± 0.10	27.3 ± 1.1	0.081 ± 0.011
s-CBZ	1.32 ± 0.05	1.01 ± 0.08	24.7 ± 0.5	0.327 ± 0.013
t-CBZ	0.452 ± 0.018	0.92 ± 0.17	23.3 ± 1.8	0.096 ± 0.013
BTI	3.962 ± 0.028	0.755 ± 0.020	30.4 ± 0.5	0.910 ± 0.021

Table S2. Photovoltaic parameters of BHJ solar cells under AM1.5G illumination (100 mW/cm^2) averaged over eight devices.

Active layer	J_{SC}, mA/cm^2	V_{OC}, V	FF, %	PCE, %
TPA:PC$_{71}$BM	7.91 ± 0.10	0.983 ± 0.009	45.0 ± 0.8	3.50 ± 0.12
m-TPA:PC$_{71}$BM	6.87 ± 0.23	0.8892 ± 0.0014	38.2 ± 0.8	2.34 ± 0.13
f-TPA:PC$_{71}$BM	8.64 ± 0.04	1.004 ± 0.010	38.5 ± 1.0	3.34 ± 0.12
s-CBZ:PC$_{71}$BM	4.95 ± 0.14	1.060 ± 0.012	30.81 ± 0.16	1.617 ± 0.029
t-CBZ:PC$_{71}$BM	2.01 ± 0.04	0.81 ± 0.12	28.2 ± 1.3	0.46 ± 0.07
BTI:PC$_{71}$BM	7.58 ± 0.10	0.936 ± 0.004	50.5 ± 1.9	3.59 ± 0.18

REFERENCES

1. R. Alvarez and G. H. Mehl, *Tetrahedron Lett.*, 2005, **46**, 67–68. (10.1016/j.tetlet.2004.11.034)

2. Z. Jiang, T. Ye, C. Yang, D. Yang, M. Zhu, C. Zhong, J. Qin and D. Ma, *Chem. Mater.*, 2011, **23**, 771–777. (10.1021/cm1018585)

3. Y. N. Luponosov, J. Min, A. N. Solodukhin, A. V. Bakirov, P. V. Dmitryakov, M. A. Shcherbina, S. M. Peregudova, G. V. Cherkaev, S. N. Chvalun, C. J. Brabec and S. A. Ponomarenko, *J. Mater. Chem. C*, 2016, **4**, 7061–7076. (10.1039/C6TC01530A)

4. S. A. Ponomarenko, N. N. Rasulova, Y. N. Luponosov, N. M. Surin, M. I. Buzin, I. Leshchiner, S. M. Peregudova and A. M. Muzafarov, *Macromolecules*, 2012, **45**, 2014–2024. (10.1021/ma2024045)

5. C. M. Cardona, W. Li, A. E. Kaifer, D. Stockdale and G. C. Bazan, *Adv. Mater.*, 2011, **23**, 2367–2371. (10.1002/adma.201004554)